ARMY RESEARCH LABORATORY

Atomic Waveguides for Atom Chips

by William M. Golding

NOTICES

Disclaimers

The findings in this report are not to be construed as an official Department of the Army position unless so designated by other authorized documents.

Citation of manufacturer's or trade names does not constitute an official endorsement or approval of the use thereof.

Destroy this report when it is no longer needed. Do not return it to the originator.

Army Research Laboratory

Adelphi, MD 20783-1197

Atomic Waveguides for Atom Chips

William M. Golding
Sensors and Electron Devices Directorate, ARL

REPORT DOCUMENTATION PAGE

1. REPORT DATE *(DD-MM-YYYY)*	2. REPORT TYPE	3. DATES COVERED *(From - To)*
October 2009	Summary/interim	

4. TITLE AND SUBTITLE	5a. CONTRACT NUMBER
Atomic Waveguides for Atom Chips	
	5b. GRANT NUMBER
	5c. PROGRAM ELEMENT NUMBER

6. AUTHOR(S)	5d. PROJECT NUMBER
William M. Golding	
	5e. TASK NUMBER
	5f. WORK UNIT NUMBER

7. PERFORMING ORGANIZATION NAME(S) AND ADDRESS(ES)	8. PERFORMING ORGANIZATION REPORT NUMBER
U.S. Army Research Laboratory ATTN: RDRL-SEE-O 2800 Powder Mill Road Adelphi, MD 20783-1197	ARL-TR-5014

9. SPONSORING/MONITORING AGENCY NAME(S) AND ADDRESS(ES)	10. SPONSOR/MONITOR'S ACRONYM(S)
	11. SPONSOR/MONITOR'S REPORT NUMBER(S)

12. DISTRIBUTION/AVAILABILITY STATEMENT

Approved for public release; distribution unlimited.

13. SUPPLEMENTARY NOTES

14. ABSTRACT

This report studies the quantum behavior of a spin one-half magnetic atom guided by a two-dimensional quadrupole magnetic field of infinite extent. The technique used is based on the Frobenius series technique and gives a complete understanding of the guide mode structure for small radial coordinates. Asymptotic solutions are used to establish boundary conditions for large radii. Various guide modes that have not been included in earlier studies are made clear by this technique. Although, in principle, the series solutions are complete, convergence is slow and the present study, therefore, uses these solutions only to establish consistent initial conditions for a differential equation solver. In this way, radial modes and eigenvalues are calculated. The results can be extended to higher spin atoms and more complicated guiding fields. These extensions along with detailed analysis of experimental limitations will be the subject of future work.

15. SUBJECT TERMS

Atom chips, atomic waveguides, BEC

16. SECURITY CLASSIFICATION OF:			17. LIMITATION OF ABSTRACT	18. NUMBER OF PAGES	19a. NAME OF RESPONSIBLE PERSON William M. Golding
a. REPORT	**b. ABSTRACT**	**c. THIS PAGE**	UU	38	19b. TELEPHONE NUMBER *(Include area code)* (301) 394-1535
Unclassified	Unclassified	Unclassified			

Contents

List of Figures

INTENTIONALLY LEFT BLANK.

1. Introduction

Atom chips are miniature structures built to control and manipulate ultracold atoms. They can be constructed using techniques borrowed from the integrated circuit, microelectromechanical systems (MEMS), and integrated optics industries. The goal is to create miniature structures that can be used to produce optical, electrical, or magnetic fields for manipulating and transporting atoms in a coherent way on a general atom chip circuit. A recent review of atom chip techniques is available in Fortágh (2007).

Some atom chip structures may be thought of as miniature versions of larger devices common in atomic physics laboratories where cold atom techniques are used. However, some devices rely on the miniature scale of the traps available on atom chips to produce quantum effects. Single mode operation of an atomic waveguide using ultracold atoms requires that the physical scale of the guiding potentials be on the order of the deBroglie wavelength of the atom. The deBroglie wavelength is inversely proportional to the atomic momentum, so to increase the wavelength the momentum of the atoms must be decreased. This is accomplished by cooling the atoms using some combination of laser cooling and magnetic evaporation. Atoms can be cooled so that their wavelengths are on the order of a few hundred nanometers. This is conveniently in the range of available lithographic and other miniature construction techniques.

A useful device that might be constructed using atom chips is the atom interferometer. A chip-based atom interferometer could be used to sense inertial fields or magnetic fields. Successful development of miniature interferometers on atom chips would allow the development of very sensitive detectors based on the interference of matter waves in cold atom systems such as Bose condensates or Fermi degenerate gases.

In one possible implementation of an atom chip-based interferometer, cold atoms would be created on the surface of an atom chip and then launched into an atom waveguide. In the waveguide, they would propagate towards a beam splitter. The splitter would be designed to cause the atomic wave packets to travel along two alternate paths through a sensing region. The atoms would then arrive at a beam combiner completing the basic interferometric structure. By counting the relative number of atoms exiting at the two output ports of the combiner (using light scattering or some other technique), a sensitive measure of the phase difference between the two alternate paths can be obtained. The main idea is that all of the necessary functions should take place on the surface of the atom chip so that a useful miniature instrument might eventually be constructed.

The phase difference between the paths in the interferometer is the basic quantity that is measured in normal operation. Many things can disturb the phase difference causing errors in the measurement. For example, local optical, electric, or magnetic fields can perturb the internal and

external atomic energy levels causing the guided atoms to accumulate phase errors. In addition, mechanical accelerations, rotations, or vibrations of the atom chip could cause relative phase errors to accumulate, disturbing the measurement. The various sources of phase error in the interferometer must be understood, controlled, and compensated for to a high level in order that very sensitive measurements can be made.

The atom waveguide in one form or another is central to the development of basic interferometric structures on atom chips. The quadrupole atom guide as well as the quantum behavior of atoms in magnetic traps has been studied by several authors (Hinds, 2000 and 2001 Bill, 2006; Lesanovsky, 2004; Sukumar, 1997; Potvliege, 2001; Bergman, 1989); however, the results of these investigations are difficult to interpret because of several problems in the analysis techniques used. It is clear that a certain class of modes may have been missed in these other works. In addition, the calculations of Hinds (2000) claim logarithmically singular solutions as physically valid guide modes for the spin one case. This is incorrect. The missing modes, singularities, and other things will be discussed here and in future work based on this analysis.

It is necessary to have a complete and correct understanding of the mode structure and the eigenvalues in order to predict various experimentally interesting properties of the magnetic guides, such as lifetime limitations or longitudinal phase shifts that may be caused by small perturbations in the fields. For example, small perturbations might be caused by limitations of the lithographic techniques currently available to construct the small wires needed. However, without a proper understanding of the behavior of the guide modes under the action of these perturbations, it is impossible to know if available construction techniques are adequate to create a useful atom guide. This report studies the quantum behavior of a spin one-half magnetic atom guided by a two-dimensional quadrupole magnetic field of infinite extent. The technique used is based on the Frobenius series technique (Ince, 1956; Bender, 1978) and gives a complete understanding of the guide mode structure for small radial coordinates. Asymptotic solutions are then used as boundary conditions at a large distance from the guide center. Although, in principle, the series solutions are complete, the present study uses these solutions only to establish consistent initial conditions for a differential equation solver. In this way, a set of radial modes and eigenvalues are calculated; however, issues pertaining to proper normalization still remain to be resolved before these modes can be used for detailed quantum calculations.

2. Magnetic Waveguides—Atom Guides using Magnetic Fields

One of the simplest types of atomic waveguides that can be constructed on an atom chip is the single-wire magnetic guide. This type of guide is designed as a single straight current-carrying wire printed lithographically on a silicon chip. The cross section of a lithographically produced wire is often nearly rectangular. Assuming the detailed cross-sectional shape of the wire can be ignored, the magnetic field created by a current flowing along the wire encircles the wire in a

right-hand sense relative to the current direction. Using large external Helmholtz coils, a uniform bias magnetic field is applied in a direction parallel to the chip surface and perpendicular to the direction of the wire. The two fields will cancel at a fixed distance above the wire creating a null in the total transverse magnetic field that extends the length of the wire. This long null in the magnetic field forms a two-dimensional quadrupole field that can be used to guide atoms along and just above the wire.

A two-dimensional finite element solution of the magnetic fields just above a rectangular current-carrying conductor is shown in figure 1. The uniform current flowing in the rectangular wire produces a magnetic field that is cancelled at about 60 µm directly above the wire surface by the field of an external pair of coils. The contour lines represent the flux density of the magnetic field and there is a magnetic null within the small circular contour. This null region is where low-field-seeking atoms will be trapped and guided in this single-wire guide design.
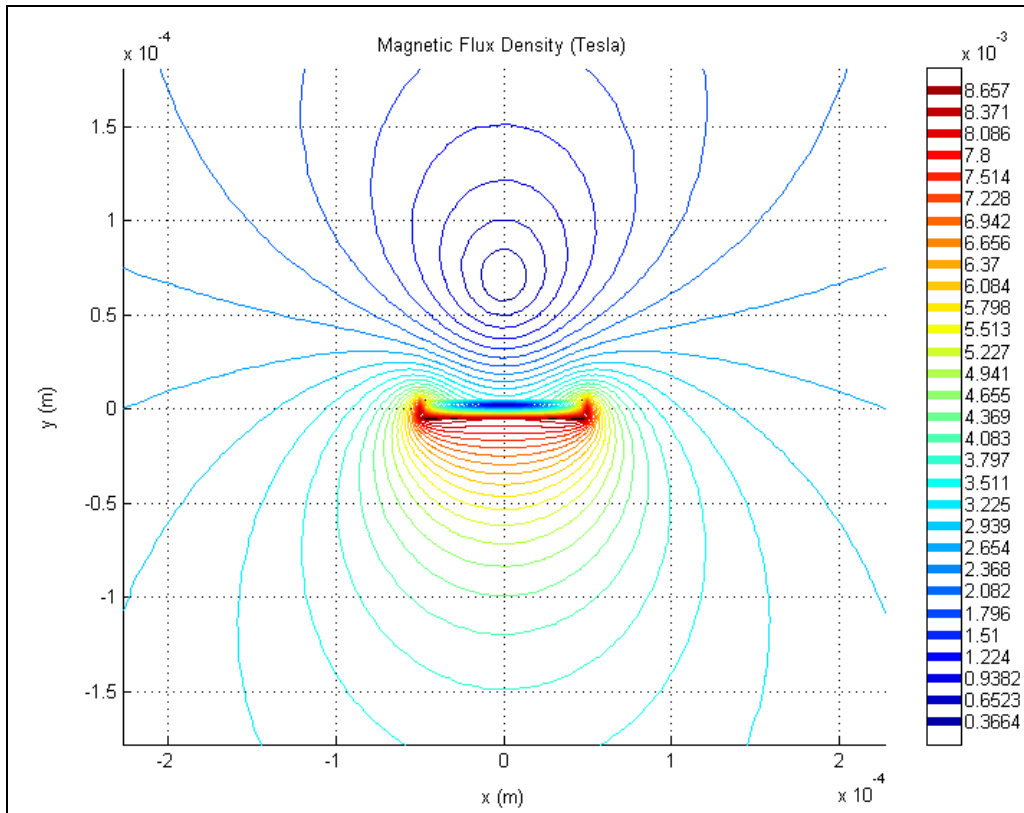
Figure 1. Cross-sectional view of the magnetic null above a single wire waveguide. Low-field-seeking atoms are guided in this local magnetic minimum.

The single-wire guide is one of the simplest structures for magnetically guiding atoms on atom chips; however, it is not an ideal guide. There are several basic difficulties that make this design inconvenient for use in general atom chip circuits. The basic problem is that the wire must be perpendicular to the fixed external bias field so that the trapping region maintains its shape and

3

strength. This means that the waveguides must be straight and run in one direction only. This is a serious design limitation for a general waveguide. Some alternative are shown in figure 2 and others are discussed in Fortágh (2007).
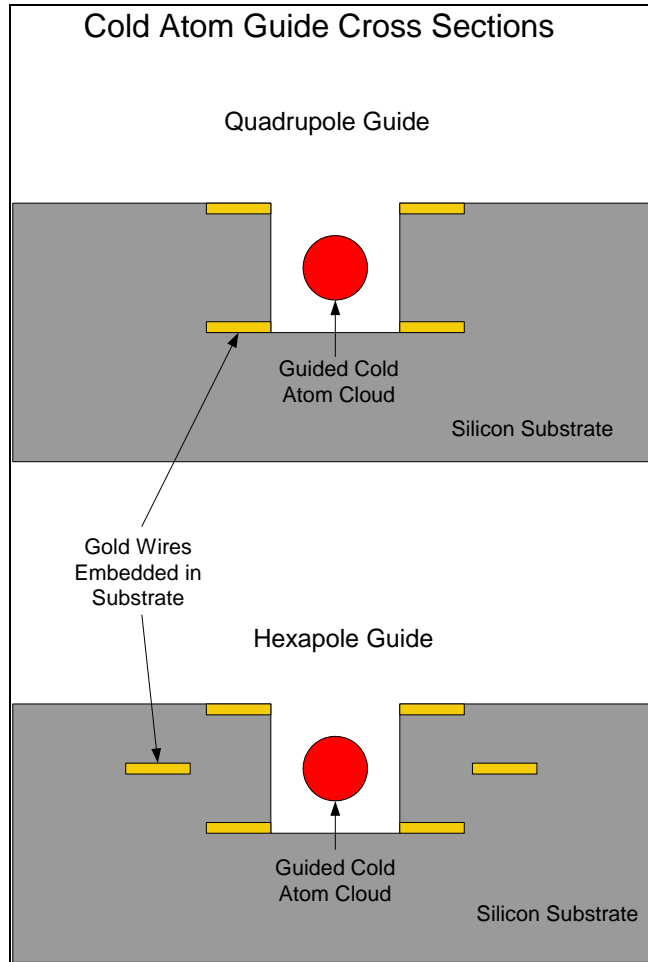
Figure 2. Two alternatives to the single-wire guide that could be constructed using etching techniques on a silicon chip. (Upper) The four-wire guide with one pair of currents going into and another pair coming out of the page, in which the current directions simply alternate from one wire to the next. The symmetry of the current distribution creates a null in the magnetic field at the center of the guide, which forms a transverse quadrupole field without the need of a large external bias coil. (Lower) A hexapole configuration shown as a simple generalization of the quadrupole guide; however, the magnitude of the potential varies quadratically from the center as opposed to the linear variation of the quadrupole. In addition, the alignment operator would be changed to $L_z - 2S_z$ instead of $L_z - S_z$.

By using multiple coplanar wires or by etching into the surface of the chip, it is possible to construct magnetic guides that can be laid out in a flexible way on the surface of an atom chip. These techniques can, in principle, produce approximate quadrupole guiding fields that twist and turn along the surface of an atom chip and preclude the need for a system of external bias coils.

Generalized quadrupole guiding structures for atoms might be used to create coherent splitters, combiners, directional couplers, and tunneling devices that are analogous designs to those presently used to create similar microwave or optical devices. However, the detailed analysis begins with the simple straight magnetic waveguide for atoms.

3. The Hamiltonian for a Straight Magnetic Waveguide

To study the dynamics of an atom in a magnetic waveguide, the Schrödinger equation describing a single neutral magnetic atom trapped in the magnetic guiding field must be solved. To minimize the initial complexities, the initial model is chosen to be a neutral spin 1/2 atomic level since it has only two magnetic levels. Although this system is essentially the same as the magnetically trapped or guided neutron, it is not completely representative of the magnetic properties of the alkali atoms that are normally used in laser cooling work. Once the study of this model atomic system is complete, a model of a more realistic system, such as the rubidium atom with $F = 1,2$, will be completed. A full model including hyperfine interactions, important in experimental systems that explore atomic clock development, could include eight or more magnetic sublevels. Rubidium is used at the U.S. Army Research Laboratory (ARL) for experimental atom chip development and a complete rubidium waveguide model will be useful for design and analysis of various experiments.

3.1 Hamiltonian for a Magnetic Atom

The quantum description of an atom moving in a spatially dependent magnetic field must include both internal and external degrees of freedom. This means that the momentum, position, and spin degrees of freedom must all be treated as quantum operators. Using m for the mass of the atom and $\vec{M}$ for the magnetic moment, the Hamiltonian is written as the sum of the kinetic energy, $\dfrac{p^2}{2m}$ and the interaction energy of the magnetic moment and the field $\vec{B}$. The result is

$$H = \frac{p^2}{2m} - \vec{M} \cdot \vec{B}(\vec{r}). \tag{1}$$

The magnetic field $\vec{B}(\vec{r})$ is independent of the *z*-direction since it is the guiding field and is taken to be an ideal quadrupole field equation (equation 2), extending to infinity in the *x-y* plane and uniform along *z*. An additional uniform bias field B_0 is added in the *z*-direction to help control possible spin-dependent losses that may occur at the zero field point at the center of the guide. The spatial dependence of the ideal quadrupole field is given by

$$\vec{B}(\vec{r}) = B_1(-x\hat{x} + y\hat{y}) + B_0\hat{z}. \tag{2}$$

A cross-sectional plot of this field is shown in figure 3. The guiding center of this field is at the origin where the transverse field is zero. The quantity B_1 is the magnitude of the transverse field gradient. It is taken as greater than or equal to zero in this work, although changing the sign of B_1 simply changes the quadrupole field configuration from one with the field point inward along the *x*-axis to one with the field pointing inward along the *y*-axis.
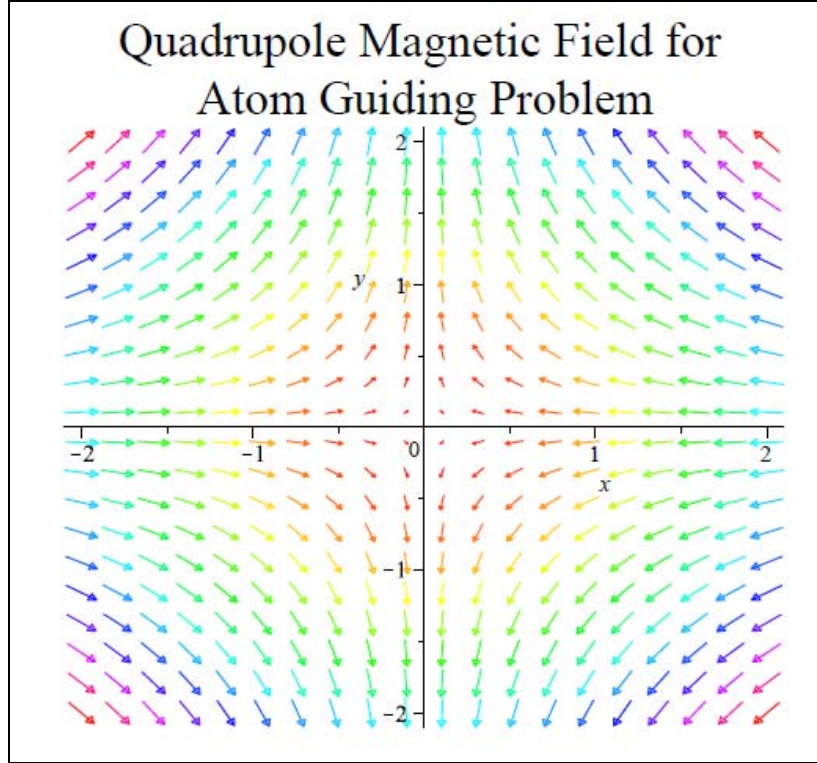
Figure 3. Cross-sectional field plot of the general quadrupole guiding field used in this work. Fields come inwards along *x* and go outwards along *y*, resulting in a quadrupole null at the center that can be used for atom guiding.

The gradient of the transverse field is what provides the trapping force that keeps the atom confined in the transverse direction. The transverse field is zero at the center of the guide and the only nonzero field component at the very center is the longitudinal bias field B_0. The magnitude of the transverse field is $|B| = B_1\sqrt{x^2 + y^2} = B_1\rho$, where ρ is the radial coordinate in the cylindrical system. Even though the field is varying in direction as one goes round the guide, the contours of constant field magnitude are simply circles.

The potential is independent of the position along the guide *z* and therefore p_z is a constant of the motion and is ignored here. In future problems, when variations in the potential along the *z*-direction are considered, the variations in the longitudinal momentum will be included. Variations in the transverse potential should show up as variations in the guide propagation constant and this will affect the accuracy of sensitive measurements based on interferometry.

6

In this simplified model of the atom (equation 1), the magnetic moment is just the magnetic moment of a single outer electron. The atomic model used here can be thought of as an alkali atom with a spin zero nucleus and a total mass m. The magnetic moment is $\vec{M} = \gamma \vec{S}$, where γ is the gyromagnetic ratio of the level considered and $\vec{S}$ is the spin angular momentum of the atom. Since a spin ½ system is being considered, the spin angular momentum is proportional to the Pauli matrices, $\vec{S} = \dfrac{\hbar}{2}\vec{\sigma}$.

The Schrödinger equation for the guided atom eigenstates $\overline{\Psi}_E$ is

$$-\frac{\hbar^2}{2M}\nabla^2 \overline{\Psi}_E(\vec{r}) - \gamma \vec{S}\cdot\vec{B}(\vec{r})\overline{\Psi}_E(\vec{r}) = E\overline{\Psi}_E(\vec{r}). \tag{3}$$

It will be solved for the energies and eigenstates. The equation 3 is made dimensionless by choosing a length scale such that $x \to \lambdabar x$, where the new x is dimensionless. Then $\dfrac{\hbar^2}{2M}\nabla^2 \overline{\Psi}_E(\vec{r}) \to \dfrac{\hbar^2 k^2}{2M}\nabla^2 \overline{\Psi}_E(\vec{r})$ and the recoil energy is defined as $E_R = \dfrac{\hbar^2 k^2}{2M}$, where $k = \dfrac{1}{\lambdabar}$ is the wavenumber of the optical field used to cool the atom. This is a rather arbitrary choice at this stage, but the recoil energy is a convenient scale for atoms that have been laser cooled. After dividing through by the recoil energy, pulling out the relevant factors, and defining the dimensionless transverse field parameter $b_1 = \gamma \dfrac{\hbar B_1 \lambdabar}{2E_R}$, the longitudinal field parameter $b_0 = \gamma \dfrac{\hbar B_0}{2E_R}$, and the scaled energy $\varepsilon = \dfrac{E}{E_R}$, the scaled Schrödinger equation becomes

$$-\nabla^2 \overline{\Psi}_\varepsilon(\vec{r}) - b_1\left(-\sigma_x x + \sigma_y y\right)\overline{\Psi}_\varepsilon(\vec{r}) - b_0\sigma_z \overline{\Psi}_\varepsilon(\vec{r}) = \varepsilon\overline{\Psi}_\varepsilon(\vec{r}). \tag{4}$$

The next step is to convert to the cylindrical coordinate system and derive the equation for the radial wave functions. In cylindrical coordinates, we have $x = \rho \cos \varphi$, $y = \rho \sin \varphi$, and the Schrödinger equation takes the following form:

$$-\nabla^2 \overline{\Psi}_\varepsilon(\rho,\varphi) + b_1\rho\left(\sigma_x \cos\varphi - \sigma_y \sin\varphi\right)\overline{\Psi}_\varepsilon(\rho,\varphi) - b_0\sigma_z \overline{\Psi}_\varepsilon(\rho,\varphi) = \varepsilon\overline{\Psi}_\varepsilon(\rho,\varphi). \tag{5}$$

Before reducing equation 5 further, an important conserved quantity in this problem will be introduced.

3.2 The Alignment Operator

The total angular momentum is not conserved in this system. Neither the orbital angular momentum $L_z \Leftrightarrow \dfrac{1}{i}\partial_\varphi$ nor the spin angular momentum $S_z \Leftrightarrow \dfrac{1}{2}\sigma_z$ individually commute with the Hamiltonian but the difference of these two operators does commute with H as shown in the

Erratum (Hinds, 2001). To show that this is the case, one can explicitly calculate the commutators of L_z and S_z with H. The appropriate operator form of the Hamiltonian for this calculation is

$$H \Leftrightarrow -\nabla^2 + b_1 \rho \left(\sigma_x \cos\varphi - \sigma_y \sin\varphi \right) - b_0 \sigma_z . \tag{6}$$

Both L_z and S_z obviously commute with the first and third terms of H, but the middle term that corresponds to the quadrupole potential is more interesting. The following straightforward calculations (equation 7) of both commutators show that they are equal to each other and nonzero unless, of course, the transverse field gradient b_1 is zero or if we consider the point $\rho = 0$.

$$
\begin{aligned}
\left[L_z, H \right] &= \frac{b_1 \rho}{i} \partial_\varphi \left(\sigma_x \cos\varphi - \sigma_y \sin\varphi \right) \\
&= i b_1 \rho \left(\sigma_x \sin\varphi + \sigma_y \cos\varphi \right) \\
\left[S_z, H \right] &= \frac{b_1 \rho}{2} \left(\left[\sigma_z, \sigma_x \right] \cos\varphi - \left[\sigma_z, \sigma_y \right] \sin\varphi \right) . \\
&= \frac{b_1 \rho}{2} \left(2 i \sigma_y \cos\varphi + 2 i \sigma_x \sin\varphi \right) \\
&= i b_1 \rho \left(\sigma_y \cos\varphi + \sigma_x \sin\varphi \right)
\end{aligned}
\tag{7}
$$

The fact that the commutators are equal means that the difference $L_z - S_z$ is a conserved quantity. For simplicity, the operator $L_z - S_z$ is relabeled as Λ_z and called the alignment operator. The alignment is obviously related to the angular momentum. Instead of being the sum of the two types of angular momentum, it is the difference. If one considers the angular momentum as a generator of rotation, then the alignment generates a coordinated rotation about the axis that maintains the angle between the field and the magnetic moment of the atom. The eigenvalues of Λ_z are denoted by μ. Since the eigenvalues of L_z are integral and the eigenvalues of S_z are half-integral in the spin ½ case, the allowed values of μ are half-integral and μ has the dimensions of an angular momentum.

Consider an atom located on the positive x-axis of the waveguide with its magnetic moment aligned with the local magnetic field. At this position the magnetic field is pointing in the negative x-direction towards the origin. If the position of the atom is rotated 90° counterclockwise around the z-axis, it will end up on the y-axis. If the rotation is performed without changing the orientation of the magnetic moment, then the moment will be perpendicular to the y-axis at this new position. This is illustrated by the red vector in figure 4. However, the quadrupole magnetic field defined in equation 2 is pointing in the positive y-direction at this position.
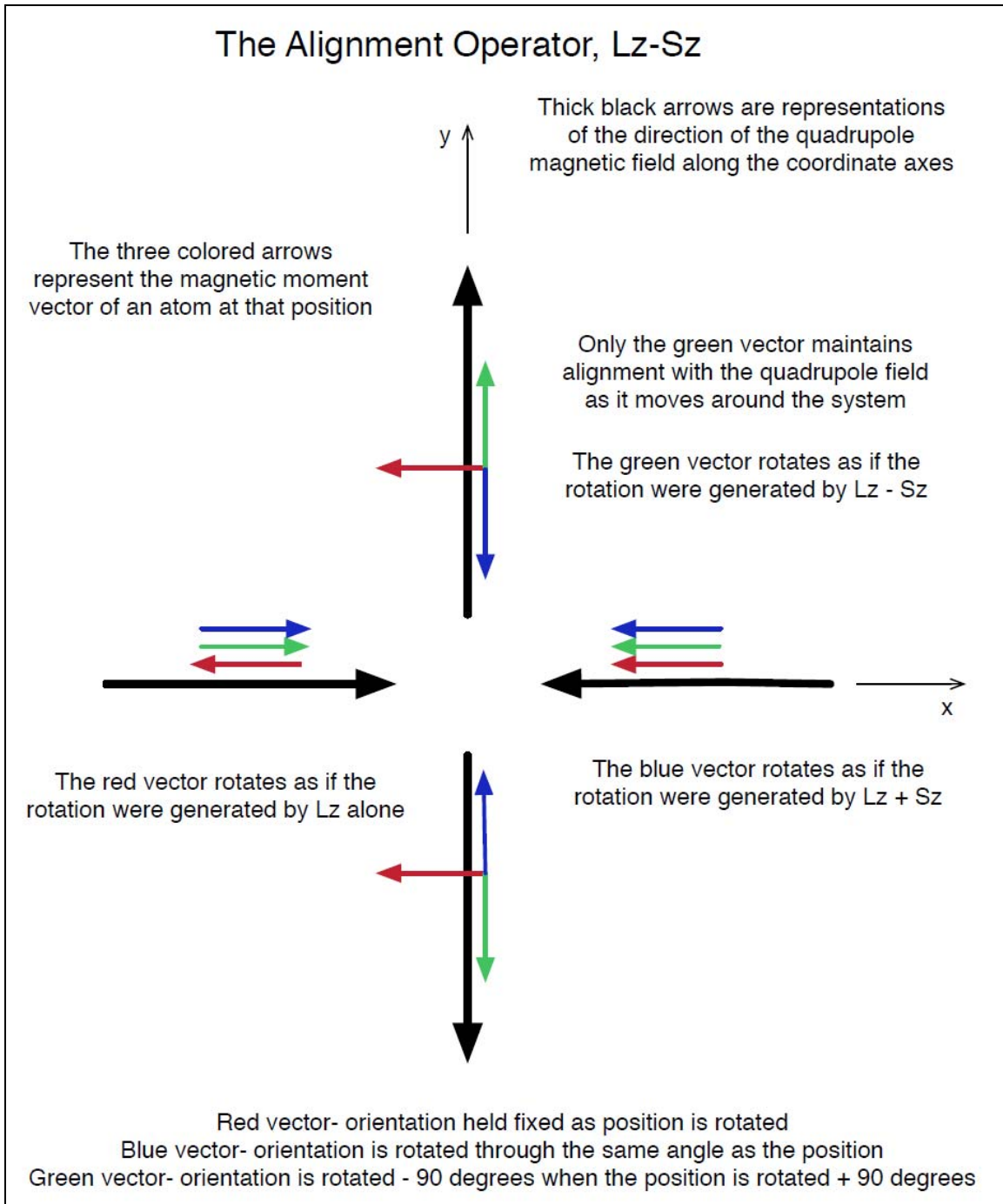
Figure 4. Illustration of the backwards rotation of the spin that must occur to keep a magnetic moment aligned with the magnetic field. The particular form of the alignment operator used here is specific to the quadrupole field.

By rotating the spin of the atom 90° clockwise, the magnetic moment will be aligned along the magnetic field as it was at the starting point on the *x*-axis. This backward 90° rotation is illustrated by the green vector in figure 4, which is always aligned with the quadrupole field as it moves around the center. The operator Λ_z is the generator of the special rotation $e^{-i\Lambda_z \theta}$ needed

to keep the spin aligned with the magnetic field, keeping the magnetic potential energy constant. It is a special property of the quadrupole field that two equal rotations of opposite sense in different spaces conserve the potential energy in this way. However, similar relations hold for higher multipole magnetic fields, in which the rotation angle of the spin must be an integer multiple of the actual rotation angle.

3.3 Eigenstates Common to H and Λ_z

Using the alignment operator, the Schrödinger equation in polar coordinates (equation 5) reduces to a radial equation for the spin components of the wave function. The first step is to rewrite the Schrödinger equation using the Pauli matrices, σ_i. The quantization axis for the spin description is the $+z$-direction and this is along the propagation axis of the guide. This basis is referred to as the global spin basis. The spin-up, ψ_+, and spin-down, ψ_-, components are referred to this global spin basis. Using the following definitions

$$-\nabla^2 \overline{\Psi}_\varepsilon (\rho,\varphi) + b_1 \rho \left(\sigma_x \cos\varphi - \sigma_y \sin\varphi \right) \overline{\Psi}_\varepsilon (\rho,\varphi) - b_0 \sigma_z \overline{\Psi}_\varepsilon (\rho,\varphi) = \varepsilon \overline{\Psi}_\varepsilon (\rho,\varphi)$$

$$\overline{\Psi}_\varepsilon (\rho,\varphi) = \begin{pmatrix} \psi_+ (\rho,\varphi) \\ \psi_- (\rho,\varphi) \end{pmatrix} \tag{8}$$

$$\sigma_x = \begin{pmatrix} 0 & 1 \\ 1 & 0 \end{pmatrix}, \quad \sigma_y = \begin{pmatrix} 0 & -i \\ i & 0 \end{pmatrix}, \quad \sigma_z = \begin{pmatrix} 1 & 0 \\ 0 & -1 \end{pmatrix}$$

in the Schrödinger equation, we arrive at the coupled system

$$\begin{pmatrix} -\nabla^2 \psi_+ (\rho,\varphi) \\ -\nabla^2 \psi_- (\rho,\varphi) \end{pmatrix} + b_1 \rho \begin{pmatrix} e^{i\varphi} \psi_- (\rho,\varphi) \\ e^{-i\varphi} \psi_+ (\rho,\varphi) \end{pmatrix} - b_0 \begin{pmatrix} \psi_+ (\rho,\varphi) \\ -\psi_- (\rho,\varphi) \end{pmatrix} = \varepsilon \begin{pmatrix} \psi_+ (\rho,\varphi) \\ \psi_- (\rho,\varphi) \end{pmatrix}. \tag{9}$$

The components are completely uncoupled if the transverse field b_1 is turned off by setting $b_1 = 0$. In this limit, the problem reduces to that of a free particle with a magnetic moment in a uniform magnetic field, b_0. Also in this limit, the operators L_z, S_z, and the alignment $\Lambda_z = L_z - S_z$ commute with H and are conserved quantities. Since these operators commute with each other as well as with H, simultaneous eigenstates can be found when $b_1 = 0$. We can use this limit as a way to identify states when the transverse field is large by allowing b_1 to reduce towards zero in the complete solutions.

The common eigenstates of L_z, S_z, and Λ_z are found using the eigenstates of L_z, S_z in the following way

$$L_z |l,m\rangle = l|l,m\rangle$$
$$S_z |l,m\rangle = m|l,m\rangle$$
$$\Lambda_z |l,m\rangle = \mu|l,m\rangle = (L_z - S_z)|l,m\rangle = (l-m)|l,m\rangle \tag{10}$$

then let $l = \mu + m$ to define simultaneous eigenstates of Λ_z,

$$\Lambda_z |\mu+m,m\rangle = \mu|\mu+m,m\rangle.$$

In the coordinate representation, $L_z \Leftrightarrow \dfrac{1}{i}\partial_\varphi$ and therefore the angular dependence of the component with alignment μ and spin m is given by $e^{i(\mu+m)\varphi}|m\rangle$. Using this angular dependence, the general multi-component wave function in the matrix representation is

$$\begin{pmatrix} \psi_+(\rho,\varphi) \\ \psi_-(\rho,\varphi) \end{pmatrix} = \begin{pmatrix} R_+(\rho)e^{i(\mu+1/2)\varphi} \\ R_-(\rho)e^{i(\mu-1/2)\varphi} \end{pmatrix}. \tag{11}$$

Although very similar, this is not the simple product form that is used in basic separation of variables techniques because the angular dependence is different for each component of the trial function. The result of using this trial form of the eigenstates in the Schrödinger equation (equation 9) is

$$\begin{pmatrix} -\nabla^2 R_+ e^{i(\mu+1/2)\varphi} \\ -\nabla^2 R_- e^{i(\mu-1/2)\varphi} \end{pmatrix} + b_1\rho \begin{pmatrix} e^{i\varphi}R_- e^{i(\mu-1/2)\varphi} \\ e^{-i\varphi}R_+ e^{i(\mu+1/2)\varphi} \end{pmatrix} - b_0 \begin{pmatrix} R_+ e^{i(\mu+1/2)\varphi} \\ -R_- e^{i(\mu-1/2)\varphi} \end{pmatrix} = \varepsilon \begin{pmatrix} R_+ e^{i(\mu+1/2)\varphi} \\ R_- e^{i(\mu-1/2)\varphi} \end{pmatrix}. \tag{12}$$

The Laplacian operator acting on the states (equation 11) produces the following terms:

$$-\nabla^2 \left(R_\pm e^{i(\mu\pm1/2)\varphi} \right) = \left(-\partial_\rho^2 R_\pm - \frac{1}{\rho}\partial_\rho R_\pm + \frac{(\mu\pm1/2)^2}{\rho^2}R_\pm \right) e^{i(\mu\pm1/2)\varphi}. \tag{13}$$

Using this expression in equation 12 results in the following system of coupled differential equations:

$$\left(-\partial_\rho^2 R_+ - \frac{1}{\rho}\partial_\rho R_+ + \frac{(\mu+1/2)^2}{\rho^2} R_+ \right) e^{i(\mu+1/2)\varphi} +$$

$$b_1 \rho e^{i\varphi} R_- e^{i(\mu-1/2)\varphi} - b_0 R_+ e^{i(\mu+1/2)\varphi} = \varepsilon R_+ e^{i(\mu+1/2)\varphi},$$

<div align="right">(14)</div>

$$\left(-\partial_\rho^2 R_- - \frac{1}{\rho}\partial_\rho R_- + \frac{(\mu-1/2)^2}{\rho^2} R_- \right) e^{i(\mu-1/2)\varphi} +$$

$$b_1 \rho e^{-i\varphi} R_+ e^{i(\mu+1/2)\varphi} + b_0 R_- e^{i(\mu-1/2)\varphi} = \varepsilon R_- e^{i(\mu-1/2)\varphi}.$$

An interesting point to notice is the way that the angular dependence factors out exactly. This cancellation is due to the way the angular factor in the quadrupole field part of the potential compensates for the action of the spin operators and is a direct consequence of using simultaneous eigenstates of H and the alignment operator Λ_z. Because of this, the angular dependence can be completely factored out of the problem leaving only the radial equations:

$$-\partial_\rho^2 R_+ - \frac{1}{\rho}\partial_\rho R_+ + \frac{(\mu+1/2)^2}{\rho^2} R_+ + b_1 \rho R_- - b_0 R_+ = \varepsilon R_+,$$

<div align="right">(15)</div>

$$-\partial_\rho^2 R_- - \frac{1}{\rho}\partial_\rho R_- + \frac{(\mu-1/2)^2}{\rho^2} R_- + b_1 \rho R_+ + b_0 R_- = \varepsilon R_-.$$

The coupled radial equations for the eigenstates of the quadrupole waveguide are shown in equation 15. They must be solved for eigenvalues and eigenvectors using the allowed half-integral values of the alignment $\mu = \pm\frac{1}{2}, \pm\frac{3}{2}, \pm\frac{5}{2}\cdots$.

As mentioned earlier, when the transverse field is turned off, the two equations in equation 15 are uncoupled. In this limit, the solutions are simply Bessel functions and they may also be common eigenstates of H, L_z, S_z, and Λ_z. Using this fact the complete solutions at $b_1 = 0$ can be written as

$$
\left| \mu, l = \mu + m, m = \tfrac{1}{2} \right\rangle \Leftrightarrow
\begin{cases}
\begin{pmatrix} J_{\mu+1/2}\left(\sqrt{(\varepsilon+b_0)}\rho\right)e^{i(\mu+1/2)\varphi} \\ 0 \end{pmatrix} & \text{bounded spin up} \\[2ex]
\begin{pmatrix} Y_{\mu+1/2}\left(\sqrt{(\varepsilon+b_0)}\rho\right)e^{i(\mu+1/2)\varphi} \\ 0 \end{pmatrix} & \text{unbounded spin up}
\end{cases}
$$

$$
\left| \mu, l = \mu + m, m = -\tfrac{1}{2} \right\rangle \Leftrightarrow
\begin{cases}
\begin{pmatrix} 0 \\ J_{\mu-1/2}\left(\sqrt{(\varepsilon-b_0)}\rho\right)e^{i(\mu-1/2)\varphi} \end{pmatrix} & \text{bounded spin down} \\[2ex]
\begin{pmatrix} 0 \\ Y_{\mu-1/2}\left(\sqrt{(\varepsilon-b_0)}\rho\right)e^{i(\mu-1/2)\varphi} \end{pmatrix} & \text{unbounded spin up}
\end{cases}
$$

(16)

The set of solutions in equation 16 represents the four free space solutions to the pair of uncoupled second order radial equations in the limit of a small transverse field, that is, when $b_1 \to 0$. It is seen that the limiting cases are clearly distinguished. There will be one mode that behaves like $J_{\mu+1/2}$ that will be referred refer to as a spin-up mode and one mode that behaves like $J_{\mu-1/2}$ that will be referred to as a spin-down mode. As the transverse field b_1 is turned on, these modes continuously evolve into modes with significant amplitudes of both components. This can be thought of as precession of a pure spin state around a transverse field. To keep things straight, the states can still be labeled by their character as $b_1 \to 0$.

As a specific example, the case of alignment ½ can be considered. In this case, the two physically acceptable solutions in the $b_1 \to 0$ limit are the spin-up J_1 state and the spin-down J_0 state. Then, to calculate the properties of the spin-down state at larger values of b_1, the series solution that reduces to J_0 spin down is used to calculate the complete behavior of the finite b_1 state near the origin. This series solution provides all initial conditions required near the origin for R_+ and R_- to initialize an ordinary differential equation (ODE) solver for the calculation of the behavior of both components of the spin-down mode at large radii.

The two solutions that involve the Bessel functions of the second kind $Y_l(\cdots)$ are unbounded at the origin and should be excluded as unphysical in problems that include the origin in the domain. This is the case in the quadrupole waveguide problem considered here. However, the unbounded solutions can be useful as they may help to identify the unphysical modes when all that is available is a complicated series solution. In the analysis by Hinds (2000) and others based on this earlier work, the two bounded modes seem to be combined into one mode, apparently leading to the use of mixed boundary conditions at the origin. For this reason, the results of that work are difficult to interpret. In this study, the modes are separately identified and

kept separate throughout the calculations. Although the scheme chosen here to separate the modes at low transverse field seems useful, more work on the effect of the various boundary conditions at the guide center is needed.

3.4   Numerical Work

Numerical techniques are used to find the eigenvalues and eigenvectors at finite b_1. The differential equation solvers that come with the Maple computer algebra system have been used in this work. The integration technique that is used is called the shooting technique and was the technique used in the work by Hinds (2000). Specific values of the parameters μ, ε, b_0, and the transverse field b_1 are chosen. An initial value is provided for both of the radial wave function components and their derivatives at the origin, and the coupled equations are integrated outwards towards large values of ρ. If the eigenvalue ε is not correct, the solution quickly grows large as an exponentially growing solution becomes dominant. The process is repeated after adjusting the eigenvalue. In this way, consistent values for the energies can be found that correspond to various modes of the guide.

However, in order to get accurate results from the differential equation solvers, accurate initial values are needed at the origin. The equations are singular at the origin and a Taylor series expansion of the general solution about the origin does not, in general, exist. The singularity at the origin is a regular singularity and series solution techniques can be used to accurately solve for the behavior of the solutions near the origin. These solutions are used to provide accurate initial conditions to the ODE solvers. In this way, specific modes that are bounded at the origin can be studied.

To obtain an equation convenient for the use of the series technique, the coupled 2nd order radial equations (equation 15) are transformed into a single 4th order equation for one specific component such as $R_+(\rho)$ of the wave function, as shown in equation 17. Once the 4th order equation is solved, the general solution for $R_+(\rho)$ contains four independent functions in series form. The four functions describing $R_-(\rho)$ are found by substitution of each $R_+(\rho)$ into equation 18. In this way, four consistent pairs of components solving the original coupled equation (equation 15) are obtained. This process can be reversed by solving first for $R_-(\rho)$ using equation 19 and then using equation 20 to find the corresponding $R_+(\rho)$ solutions.

Solving in either order produces a valid general solution to the system, but often one way produces a better form for the resulting solutions. This can be a useful way to identify log free regular solutions to the system. These types of solutions are free from singularities at the origin and are the physical solutions required in the waveguide problem under study.

14

$$\rho^4 \frac{d^4}{d\rho^4} R_+ +$$

$$\left[2\rho^4 \varepsilon - \left(\frac{5}{2} + 2\mu^2 \right) \rho^2 \right] \frac{d^2}{d\rho^2} R_+ +$$

$$\left[-2\rho^3 b_0 + \left(5 + 4\mu^2 + 6\mu \right) \rho \right] \frac{d}{d\rho} R_+ +$$

$$\left[-b_1^2 \rho^6 + \left(\varepsilon^2 - b_0^2 \right) \rho^4 + \left(b_0 - 2\mu^2 \varepsilon + 2\mu b_0 + \frac{1}{2} \varepsilon \right) \rho^2 - \frac{19}{2} \mu^2 - 9\mu - \frac{35}{16} + \mu^4 \right] R_+ = 0$$

(17)

$$R_-(\rho) = \frac{1}{b_1 \rho} \left\{ \frac{d^2}{d\rho^2} R_+(\rho) + \frac{\frac{d}{d\rho} R_+(\rho)}{\rho} - \frac{\left(\mu + \frac{1}{2} \right)^2 R_+(\rho)}{\rho^2} + \left(\varepsilon + b_0 \right) R_+(\rho) \right\}$$

(18)

$$\rho^4 \frac{d^4}{d\rho^4} R_- +$$

$$\left[2\rho^4 \varepsilon - \left(\frac{5}{2} + 2\mu^2 \right) \rho^2 \right] \frac{d^2}{d\rho^2} R_- +$$

$$\left[2\rho^3 b_0 + \left(5 + 4\mu^2 - 6\mu \right) \rho \right] \frac{d}{d\rho} R_- +$$

$$\left[-b_1^2 \rho^6 + \left(\varepsilon^2 - b_0^2 \right) \rho^4 + \left(-b_0 - 2\mu^2 \varepsilon + 2\mu b_0 + \frac{1}{2} \varepsilon \right) \rho^2 - \frac{19}{2} \mu^2 + 9\mu - \frac{35}{16} + \mu^4 \right] R_- = 0$$

(19)

$$R_+(\rho) = \frac{1}{b_1 \rho} \left\{ \frac{d^2}{d\rho^2} R_-(\rho) + \frac{\frac{d}{d\rho} R_-(\rho)}{\rho} - \frac{\left(\mu - \frac{1}{2} \right)^2 R_-(\rho)}{\rho^2} + \left(\varepsilon - b_0 \right) R_-(\rho) \right\}$$

(20)

Each of the 4th order equations 17 and 19 are solvable using the Frobenius technique for higher order equations (Ince, 1956; Bender, 1978). The basic idea is to use a modified power series form for the solution and to solve for the unknown coefficients. An assumed series solution of the form

$$R_+(\rho) = \sum_{\nu=0}^{\infty} c_\nu \rho^{s+\nu}$$

(21)

is used in one of the 4th order equations. The coefficients c_ν and the index s are determined by equating the coefficients of like powers on either side of the equation to zero. The first equation will be of the form $c_0 f_0(s) = 0$ and c_0 is assumed equal to one. The equation $f_0(s) = 0$ is called the

15

indicial equation and there are four roots s_i. Each root corresponds to one solution of one of the differential equations 17 or 19. The indicial equations and the roots are both given as follows:

$$R_+ \Rightarrow s^4 - 6s^3 + \left(\frac{17}{2} - 2\mu^2\right)s^2 + \left(\frac{3}{2} + 6\mu^2 + 6\mu\right)s - 9\mu - \frac{35}{16} + \mu^4 - \frac{19}{2}\mu^2 = 0,$$

(22)

$$s = \mu + 1/2, \ -\mu + 7/2, \ -\mu - 1/2, \ \mu + 5/2.$$

$$R_- \Rightarrow s^4 - 6s^3 + \left(\frac{17}{2} - 2\mu^2\right)s^2 + \left(\frac{3}{2} + 6\mu^2 - 6\mu\right)s + 9\mu - \frac{35}{16} + \mu^4 - \frac{19}{2}\mu^2 = 0,$$

(23)

$$s = -\mu + 1/2, \ \mu + 7/2, \ \mu - 1/2, \ -\mu + 5/2.$$

In the case of $\mu = 1/2$, the indices for the R_+ equation are $s_+ = (3,3,1,-1)$ and for the R_- equation the indices are $s_- = (4,2,0,0)$. The largest index always produces a solution free from logarithms in the Frobenius method and is thus bounded at the origin. Thus, two types of log-free modes with leading behaviors of $R_+ \sim \rho^3$ and $R_- \sim \rho^4$ at the origin are found.

Since μ must be half integral, the solutions to the indicial equations are all integers. This is a special case in the Frobenius technique that results in some of the series solutions containing logarithmic terms like $\ln(\rho)$ times another power series. These logarithmic terms are unbounded unless multiplied by a positive power of ρ. They must be excluded from the physical solutions if they cause either component of the solution to become unbounded.

In the modes studied so far, two bounded and two unbounded solutions are always found by this technique for any value of μ. This should be expected by examining the limiting behavior of the solutions demonstrated in equation 16 for small values of b_1. Since b_1 and ρ are independent, any logarithmic terms in ρ cannot simply be cancelled by allowing $b_1 \rightarrow 0$.

However, there are cases when straightforward application of the series technique apparently results in only one solution that is bounded at the origin, the other three being unbounded. The four solutions together must represent the general solution to the problem. By inspecting the limiting forms (equation 16), a linear superposition of the three unbounded solutions can be constructed to create two unbounded and one bounded solution, again resulting in two independent bounded solutions. Essentially, a singularity present in two of the calculated series is cancelled by this technique producing the additional regular log free solution.

Once the series solutions (equation 21) for various values of s are determined, they are individually substituted into the corresponding equation (equation 18) to obtain the related series solution for the other solution. In this way, four consistent pairs of series solutions are generated for the system (equation 15).

These four functions together represent a fundamental solution to the waveguide problem for a particular value of the alignment eigenvalue μ. Two modes are bounded and two are unbounded at the origin, as mentioned previously. The series solutions do not converge quickly for large distances from the guide center and the basic requirement in the search for eigenvalues is that solutions remain bounded at large radii as well as at the origin. A better technique for large radii is to use an ODE solver and integrate outwards from the origin. The series solutions are ideal tools to establish consistent initial conditions at some point away from the origin so that the singularities do not negatively affect the ODE solver.

Samples of the four series solutions obtained via the Frobenius technique for the case $\mu = 1/2$ are displayed in equations 24 through 27. The solutions are labeled $Rms1$, etc., indicating series one for R_- and so on. The series labeled $Rps1$, etc., are derived directly from the corresponding Rm series using equation 20. The bounded solutions in this case are $Rms1$ and $Rms3$ and these series are the basis of two types of waveguide modes that are distinguished by their behavior at the origin.

For the case $\mu = 1/2$ the allowed values of s_- are (4,2,0,0). $Rms1$ is the solution with the indicial exponent 4. This is the largest exponent of the group and, therefore, $Rms1$ is finite at the origin according to the Frobenius theory (Ince, 1956; Bender, 1978). Both components of the $Rms1$ solution are zero at the origin, which may lead to an inherent insensitivity to certain types of spin flips or field fluctuations that are possible at the zero field point at the guide center. As $b_1 \to 0$ the component $Rps1$ dominates and the combination behaves like the $|m = 1/2\rangle$ spin-up state identified in equation 16. This is how the states are identified for arbitrary b_1.

$$Rms1 = \left(\frac{1}{4800} b_1^2 - \frac{1}{23040} \varepsilon^3 \right) \rho^{10} + \frac{1}{384} \varepsilon^2 \rho^8 - \frac{1}{12} \varepsilon \rho^6 + \rho^4$$

$$(24)$$

$$Rps1 = \frac{1}{115200} \frac{\left(24\varepsilon b_1^2 - 5\varepsilon^4 \right) \rho^9}{b_1} + \frac{1}{115200} \frac{\left(2400 b_1^2 - 200\varepsilon^3 \right) \rho^7}{b_1} + \frac{1}{12} \frac{\rho^5 \varepsilon^2}{b_1} - 2 \frac{\rho^3 \varepsilon}{b_1} + 16 \frac{\rho}{b_1}$$

The solution $Rms2$ is the $s = 2$ solution and both components have logarithmic terms that are multiplied by positive powers of ρ. These terms are actually finite at the origin, but the $1/\rho$ term in $Rps2$ is unbounded so this term must be excluded from the physical solutions. The singularity in $Rps2$ comes from substituting $Rms2$ into the differential equation 20. The derivative of the log produces the singularity.

$$Rms2 = \left(-\frac{1}{3072} \rho^8 \varepsilon^3 + \frac{1}{96} \rho^6 \varepsilon^2 - \frac{1}{8} \rho^4 \varepsilon \right) \ln(\rho) +$$

$$\left(\frac{1}{1536} b_1^2 - \frac{7}{5760} \varepsilon^3 \right) \rho^8 + \frac{83}{1920} \rho^6 \varepsilon^2 - \frac{299}{480} \rho^4 \varepsilon + \rho^2$$

(25)

$$Rps2 = \left(-\frac{1}{3072} \frac{\varepsilon^4 \rho^7}{b_1} - \frac{1}{96} \frac{\varepsilon^3 \rho^5}{b_1} + \frac{1}{4} \frac{\varepsilon^2 \rho^3}{b_1} - 2 \frac{\varepsilon \rho}{b_1} \right) \ln(\rho) +$$

$$\frac{1}{46080} \frac{\left(-56\varepsilon^4 + 30\varepsilon b_1^2 \right) \rho^7}{b_1} + \frac{1}{46080} \frac{\left(1920 b_1^2 - 1832\varepsilon^3 \right) \rho^5}{b_1} + \frac{127}{120} \frac{\varepsilon^2 \rho^3}{b_1} - \frac{299}{30} \frac{\varepsilon \rho}{b_1} + \frac{4}{b_1 \rho}$$

The indicial exponent $s = 0$ produces the solution $Rms3$. This solution is an acceptable solution that is nonzero at the origin. However, it also behaves as $R_+ \rightarrow J_1\left(\sqrt{\varepsilon}\rho \right)$ for small values of b_1 and could also be a $|m = 1/2\rangle$ state. Closer inspection shows that the pair of solutions generated by the $b_1 \rightarrow 0$ limit can be created as superpositions of the $Rms1$ and $Rms3$ series. For example, the series $RMS3$ in equation 26 should be $J_0\left(\sqrt{\varepsilon}\rho \right)$. The two leading terms are correct but a term proportional to ρ^4 is missing. Since the leading term of $Rms1$ in equation 24 is also ρ^4 these series can be added to fill in the missing term. This produces both a modified $Rms3$ and a modified $Rps3$ of precisely the correct limiting behavior. This type of correction is currently done by hand for the various series generated at different values of alignment; however, a general way of combining and creating solutions to automatically obtain the desired limiting behavior for various values of μ is being developed. This will enhance the usefulness of any results based on these modes.

$$Rms3 = \left(\frac{1}{288} b_1^2 + \frac{1}{1152} \varepsilon^3 \right) \rho^6 - \frac{1}{4} \rho^2 \varepsilon + 1$$

(26)

$$Rps3 = -\frac{1}{1152} \frac{\left(-4\varepsilon b_1^2 - \varepsilon^4 \right) \rho^5}{b_1} - \frac{1}{1152} \frac{\left(-36\varepsilon^3 - 144 b_1^2 \right) \rho^3}{b_1} - \frac{1}{4} \frac{\varepsilon^2 \rho}{b_1}$$

The solution $Rms4$ also contains logarithmic terms and is unbounded at the origin. It is not a physically acceptable solution as it has a term proportional to $\frac{1}{\rho}$.

$$Rms4 = \left(\left(\frac{1}{816}b_1^2 + \frac{1}{3264}\varepsilon^3\right)\rho^6 - \frac{3}{34}\rho^2\varepsilon + \frac{6}{17}\right)\ln(\rho) +$$

$$\left(\frac{7}{3264}b_1^2 + \frac{5}{6528}\varepsilon^3\right)\rho^6 - \frac{9}{1088}\rho^4\varepsilon^2 - \frac{2}{17}\rho^2\varepsilon + 1$$

$$Rps4 = \left(-\frac{1}{6528}\frac{\left(-2\varepsilon^4 - 8\varepsilon b_1^2\right)\rho^5}{b_1} - \frac{1}{6528}\frac{\left(-72\varepsilon^3 - 288b_1^2\right)\rho^3}{b_1} - \frac{3}{34}\frac{\varepsilon^2\rho}{b_1}\right)\ln(\rho) -$$

$$\frac{1}{6528}\frac{\left(-14\varepsilon b_1^2 - 5\varepsilon^4\right)\rho^5}{b_1} - \frac{1}{6528}\frac{\left(-150\varepsilon^3 - 600b_1^2\right)\rho^3}{b_1} - \frac{1}{4}\frac{\varepsilon^2\rho}{b_1} + \frac{3}{17}\frac{\varepsilon}{b_1\rho}$$

(27)

4. Farfield Solutions

The coupled equation 15 can be solved approximately in the limit as $\rho \to \infty$. This is accomplished by ignoring terms that are small relative to the linearly increasing term proportional to b_1. The resulting approximate equation is independent of μ, ε, and b_0. It has the following solutions:

$$R_-(\rho) = C_1 I_0\left(\frac{2}{3b_1}(b_1\rho)^{\frac{3}{2}}\right) + C_2 J_0\left(\frac{2}{3b_1}(b_1\rho)^{\frac{3}{2}}\right) + C_3 K_0\left(\frac{2}{3b_1}(b_1\rho)^{\frac{3}{2}}\right) + C_4 Y_0\left(\frac{2}{3b_1}(b_1\rho)^{\frac{3}{2}}\right)$$

$$R_+(\rho) = C_1 I_0\left(\frac{2}{3b_1}(b_1\rho)^{\frac{3}{2}}\right) - C_2 J_0\left(\frac{2}{3b_1}(b_1\rho)^{\frac{3}{2}}\right) + C_3 K_0\left(\frac{2}{3b_1}(b_1\rho)^{\frac{3}{2}}\right) - C_4 Y_0\left(\frac{2}{3b_1}(b_1\rho)^{\frac{3}{2}}\right)$$

(28)

The only unacceptable solution at ∞ is the I_0 solution. By adding and subtracting these two equations, the oscillatory and exponential terms are isolated. The resulting equations are

$$R_+(\rho) + R_-(\rho) = C_1 I_0\left(\frac{2}{3b_1}(b_1\rho)^{\frac{3}{2}}\right) + C_3 K_0\left(\frac{2}{3b_1}(b_1\rho)^{\frac{3}{2}}\right)$$

$$R_+(\rho) - R_-(\rho) = C_2 J_0\left(\frac{2}{3b_1}(b_1\rho)^{\frac{3}{2}}\right) + C_4 Y_0\left(\frac{2}{3b_1}(b_1\rho)^{\frac{3}{2}}\right)$$

(29)

The physical basis of this behavior is that expressions $R_+(\rho) \pm R_-(\rho)$ are proportional to the two components of the eigenstates of S_x and the magnetic field is aligned with the x-axis at $\varphi = 0$. The components $R_+(\rho) \pm R_-(\rho)$ form the components of what is called the local basis in the section 5. These two components then exhibit purely bound or purely unbound behavior.

19

Physically acceptable solutions are obtained only for $C_1 = 0$, thus the sum $R_+(\rho) + R_-(\rho)$ decays as $K_0\left(\dfrac{2}{3b_1}(b_1\rho)^{3/2}\right)$ for $\rho \to \infty$. This is the basis of the procedure to find the eigenvalues, ε. The equations are integrated using an ODE routine for various values of ε. The correct eigenvalues are the ones that effectively force $C_1 = 0$ producing the physical boundary condition $R_+(\rho) + R_-(\rho) \to 0$ for $\rho \to \infty$. In the section 5, many samples of these eigenstates and eigenenergies are discussed.

5. Numerical Solutions

In this section, the results of the numerical techniques described in the text are displayed for various parameters. The components $R_+(\rho) \pm R_-(\rho)$ discussed in the text form the components of the local basis. The components in the local basis are labeled by $R_s = R_+ + R_-$ and $R_d = R_+ - R_-$. This pair of components is what is meant by local basis components in the text of this section. The component R_s is proportional to the amplitude for the spin to be pointed along the positive x direction and R_d is proportional to the amplitude for the spin to be found pointing in the negative x-direction. Since the magnetic field is chosen to be pointing along the negative x-direction and the spin is chosen to be parallel to the magnetic moment, the R_s component of the wavefunction is aligned opposite to the magnetic field and must act as a bound component at large radii where the magnitude of the magnetic field gets very large. Since the R_d component is aligned with the field, it must be unbound as the effective magnetic potential energy decreases for large radii.

The solutions, therefore, are of a peculiar nature in that one component in the local basis appears to be a localized bound state yet the other component extends to infinity. This makes it difficult to identify solutions that can be considered to be purely bound states. However, the solutions for $\pm\mu$ form a degenerate pair when $b_0 = 0$. This means that the solution found for one value of μ is only one component of a degenerate pair of solutions. Any linear superposition of these two states is then also a solution with the common eigenvalue. It turns out that by simply adding and subtracting the two degenerate solutions, a new set of degenerate states that are either purely bound or purely unbound states can be formed.

In this way, the solutions are separated into bound and unbound pairs. The bound states are concentrated near the center of the guide, decaying exponentially away from the guide axis and the unbound states oscillate and extend to infinity. The modes of interest in atom guiding are the bound modes, as the unbound modes will tend to interact with things far from the guide center and thereby be easily lost from the guide. However, the bound and unbound modes are degenerate and it will be difficult experimentally to keep them from mixing with each other and eventually causing atoms to be lost from the guide. The introduction of a nonzero bias field b_0 can remove the degeneracy, leaving isolated bound and unbound modes. This is analogous to the

20

introduction of a bias field in magnetic traps to reduce spin flips in the adiabatic approximation. The details of this connection with the adiabatic picture will be a subject of future study.

In figure 5, the degenerate low energy states of the modes with zero axial amplitudes are shown in the global basis. On the left of figure 5, the mode with $\mu = 1/2$ is shown, and on the right, the degenerate mode for $\mu = -1/2$ is shown. For zero bias field, these modes are identical except for the exact reversal of the roles of R_+ and R_-.
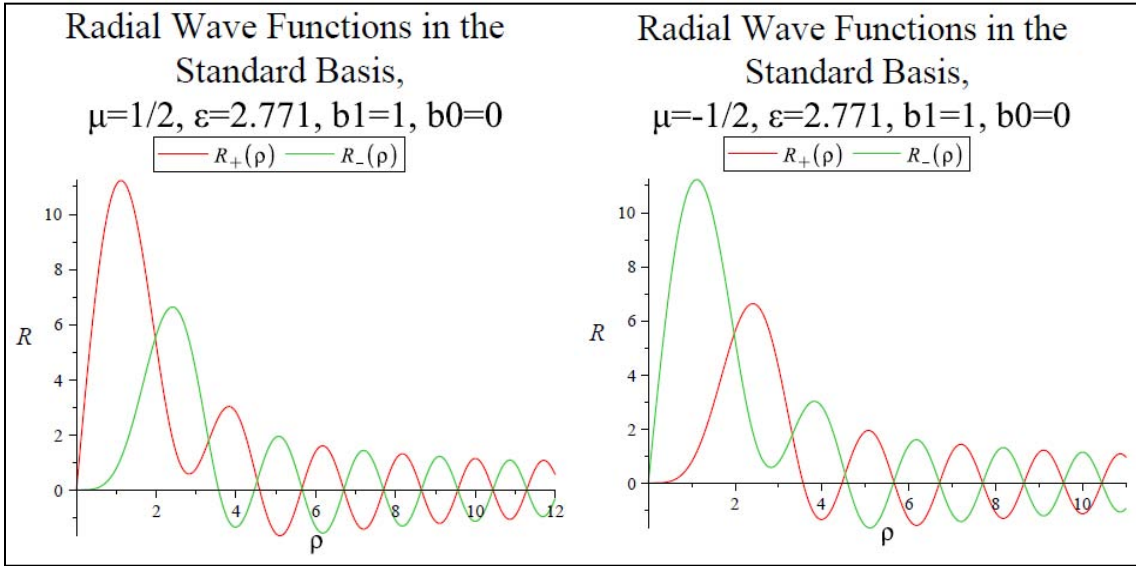
Figure 5. These plots show a μ = 1/2 eigenstate (left) and the μ = –1/2 degenerate eigenstate (right). The mode on the left is spin up in the low field limit and the mode on the right is spin down in this limit. Notice that the two components in each mode oscillate as out of phase Bessel functions at large radius and that the roles of R$_+$ and R$_-$have been reversed relative to each other. The fact that these two modes are degenerate allows them to be combined to form pure bound or unbound states.

In figure 6, the same modes shown in figures 5 are displayed except they are now both in the local basis. The bound component of each of these modes is apparent as the red curve that decays at large radius. However both modes are clearly mixed with bound and unbound components that oscillate as $\rho \to \infty$. Since these modes are degenerate, they can be cleanly separated into bound and unbound modes by simply superpositioning the degenerate pair. By adding and subtracting the modes from one another, new modes are formed that each contains a single nonzero component and one component that is identically zero. It is not simply the individual sum and difference of spin components that takes the mode from the global to the local spin basis but a superposition of two degenerate modes both of which are in the local spin basis. The result of combining the modes is shown in figure 7. Only one component is visible in each of these plots because the other component has been exactly cancelled out. Since this separation into bound and unbound modes is based on the degeneracy of the $\mu = \pm 1/2$, modes that occurs when $b_0 = 0$

it is expected that nonzero values of b_0 will lift the degeneracy and provide a purely quantum description of the stabilizing effect of the bias field in magnetic traps. A complete study of this effect and a comparison with the adiabatic approximation will be the subject of a future study.
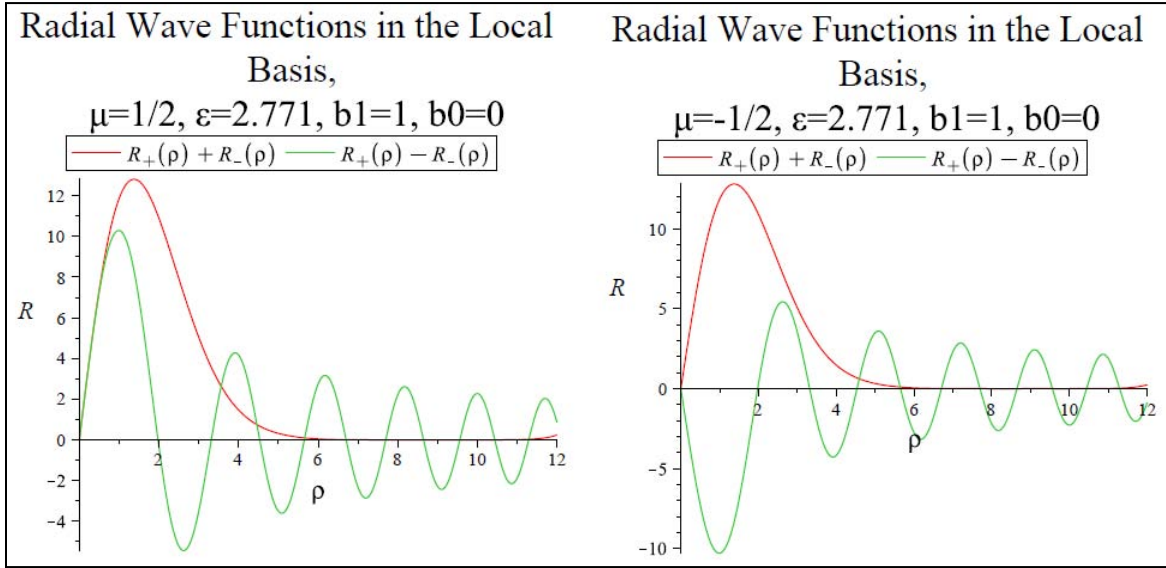

Figure 6. Local basis eigenstates corresponding to the global basis states shown in figure 5. The components of the local basis states are derived from the global states by forming the sum and difference of the global components. This can also be accomplished as a basis transformation using rotation matrices to go from the S_z to S_x basis. The significant difference between the local and global basis representations is the appearance of an exponentially decaying bound component along with an oscillatory or unbound component. The bound components in the two degenerate modes are equal and have the same sign, but the unbound components have opposite signs. For this reason the sum and the difference of the two degenerate modes can be used to produce pure bound and unbound states as shown in figure 7.
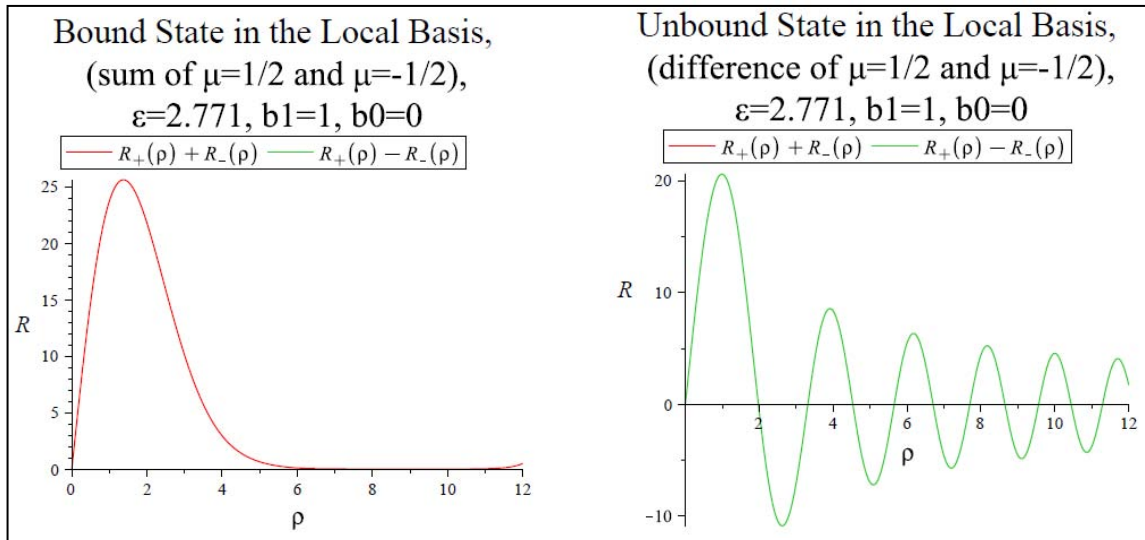
Figure 7. Purely bound state obtained by forming a superposition of the degenerate states shown in figure 6.

22

The first higher order local mode for the $\mu = \pm 1/2$ case is displayed in figure 8. This is the second mode in the series of modes that behave like J_1 at low transverse field. The bound component, shown in red, clearly crosses the axis once and returns exponentially to zero from negative values. The unbound modes, shown in green, oscillate in a manner similar to a Bessel function, but these two components are clearly exactly out of phase for the two different values of μ. This behavior is the same in all degenerate pairs and again allows the formation of pure bound and unbound modes. In figure 9, the next two higher order modes of this sequence are displayed. It is clear that the bound components are behaving in the same way as in other quantum mechanical bound state problems. The difference here is the intermingling of the bound and unbound behavior within one mode and is due to the extra spin degree of freedom not found in the more common potential well problems that involve scalar particles. This makes the identification of pure bound states difficult.
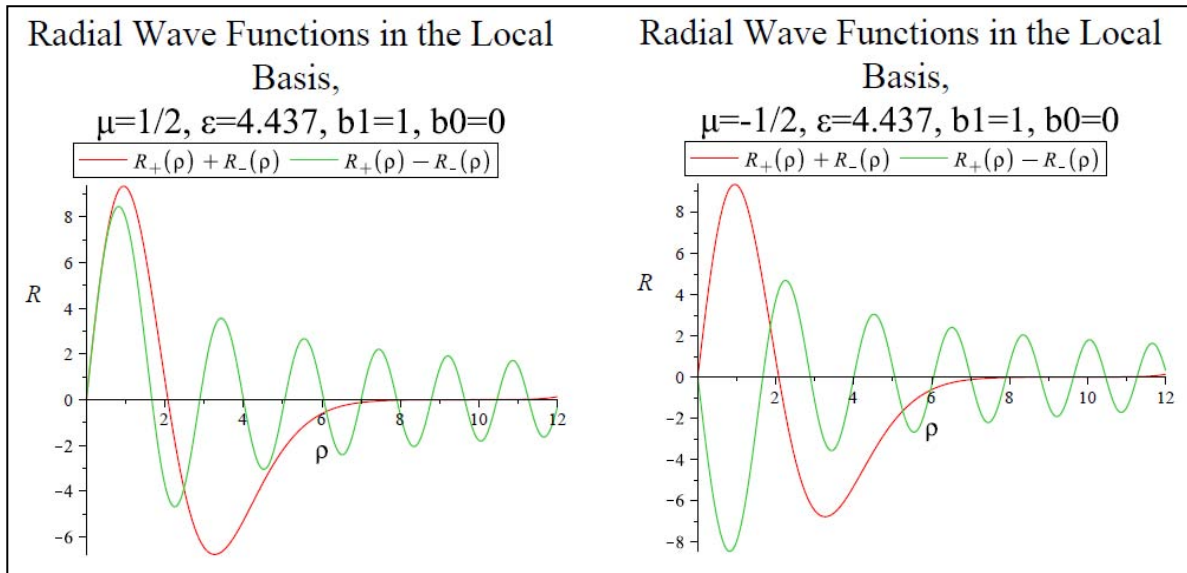
Figure 8. These two states are the degenerate pair of the first excited modes in the system of modes that act like J_1 when the transverse field goes to zero. Since they are degenerate, they can be combined to obtain pure unbound and bound modes.
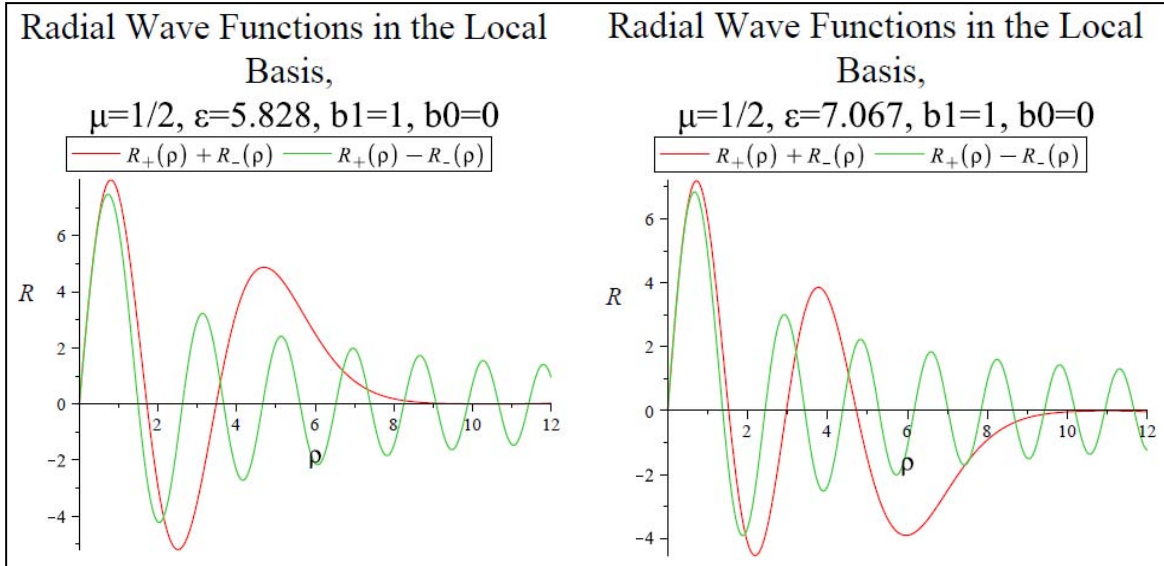
Figure 9. These are the next two higher order modes in the system of modes that act like J_1 when the transverse field goes to zero. As expected, the number of zero crossings increases as the mode energy increases.

The second sequence of modes behaves like J_0 at the origin. These lowest of these modes are lower in energy than the J_1 type modes and should be considered the ground state of the system. This apparent ground state is shown in figure 10. This mode may have some contamination in it as discussed in section 3. We are currently developing a way to exclude these types of contamination so that a complete and systematic study of all the modes can be completed. Another issue may be that this ground state designation is system dependent, as the differing behavior of these modes at the origin might be used along with various mode suppression strategies to eliminate some levels, possibly including the original ground state. In figure 11, a few higher modes of this sequence are displayed in the local basis. In the local basis, both components of the $\mu = \pm 1/2$ modes are nonzero at the origin. In figure 12, the lowest energy state for the $\mu = 3/2$ case is presented. Its bound state component also has no zero crossings and could be considered a ground state for atoms constrained to be in the $\mu = 3/2$ state of alignment.
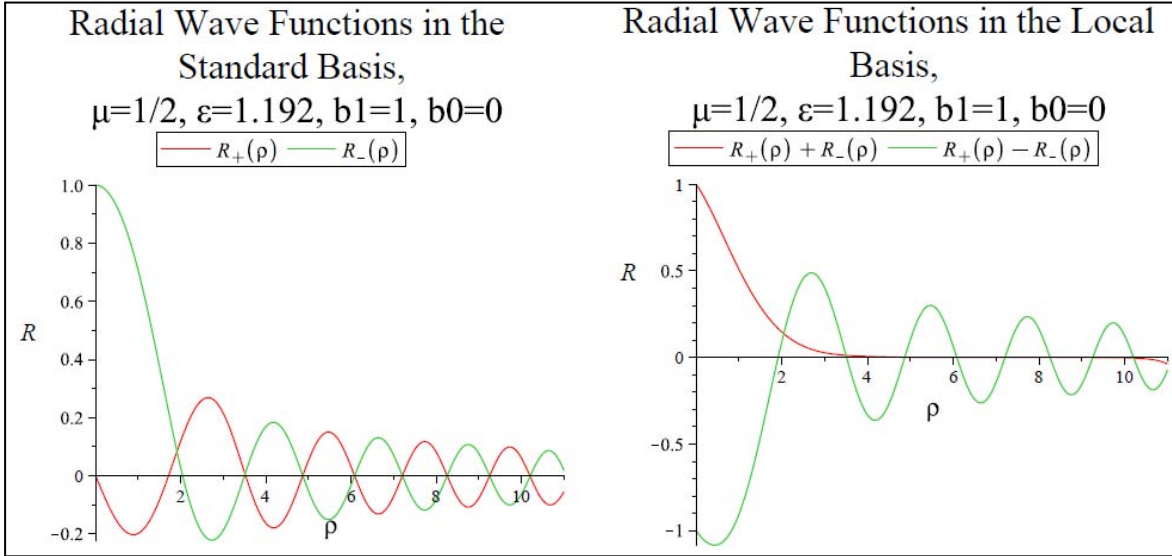
Figure 10. This state is the lowest order mode of the system of modes that behave like J_0 as the transverse field is decreased. Notice the large on axis component that distinguishes this mode from the J_1 type modes. This mode is the likely ground state of the system; however, there is some mixing of modes from the spin-up solutions in this system as discussed in the text of section 3. Thus, this mode might represent a superposition of spin-up and spin-down eigenstates. It is shown in both the global and local bases.
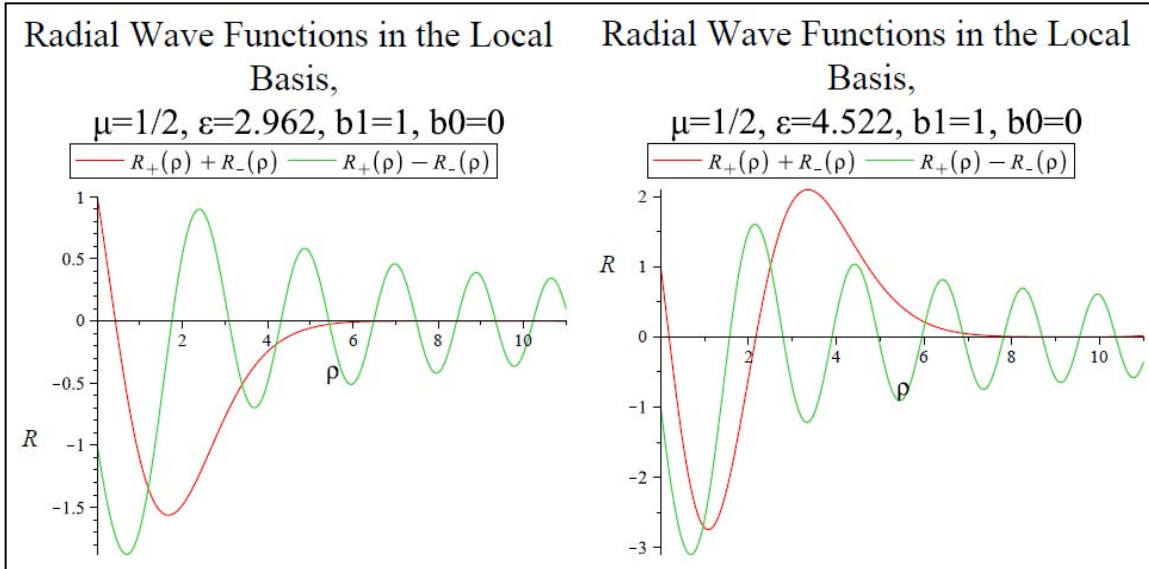
Figure 11. Local behavior of the higher order modes that behave like J_1 and J_2 at low transverse field
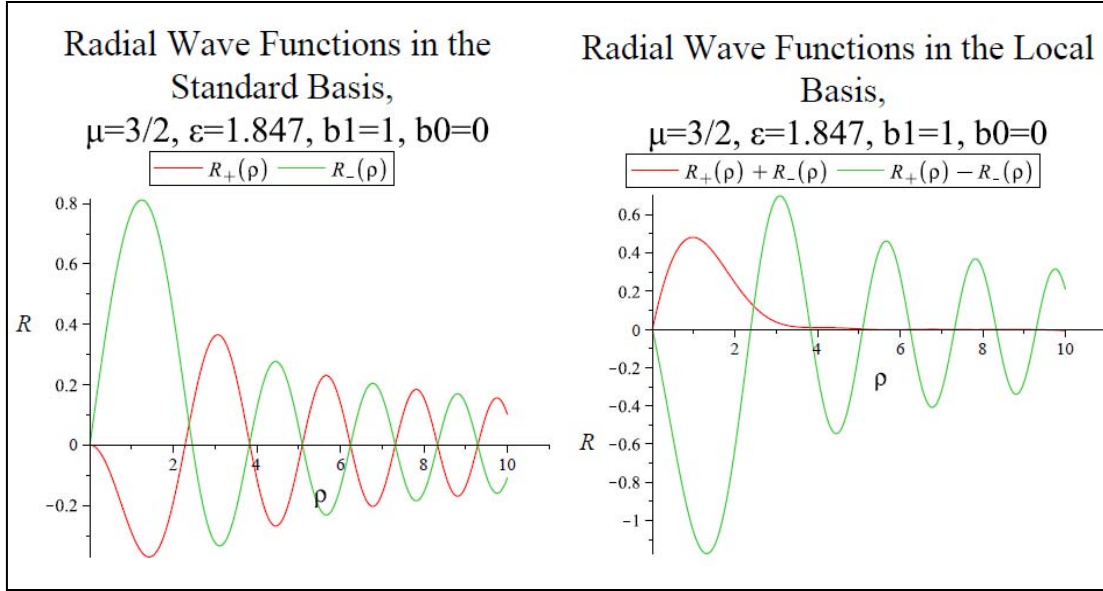
Figure 12. These two plots for the lowest energy $\mu = 3/2$ state show that the same basic behavior holds for alignment other than $\mu = \pm 1/2$. The solutions can be found for higher values of alignment as well.

6. Conclusions

A technique for solving for the eigenmodes and eigenvalues of the magnetic quadrupole waveguide has been developed. The technique is robust, but there is still some room for improvement. A good understanding of the modes and mode structure has been obtained; however, the numerical techniques being used for the calculations can still produce some contamination between modes that can result in errors in the calculated energies. This is currently being resolved and an improved technique will be incorporated soon.

The calculated modes are of a peculiar nature that is not completely bound or completely unbound, which causes a problem as they are not strictly normalizeable. Rather, the modes are of a hybrid nature. A possible resolution of this problem is to use degeneracy to split the hybrid modes into pure bound and pure unbound states. This technique appears to be useful, but we are still left with modes that must be normalized properly to be used in further calculations. A reliable technique to handle this problem for the hybrid modes has not yet been developed. It may be the case that some type of box normalization could be useful for the unbound states, but this would have to include the bound states in some natural way so that consistent expectations could be calculated. Another issue is the possible close coupling of the degenerate bound and unbound states. This coupling could cause possible lifetime limitations. This degeneracy must be studied and the usefulness of the bias field in lifting the degeneracy in a purely quantum

situation, reducing any related decay mechanisms, must be considered. Some details still need to be resolved, but as the remaining issues are cleared up these mode calculations will be useful for further calculations of important effects in the use of atomic waveguides in atom interferometry based on atom chips.

7. References

Bender, C. M.; Orszag, S. A. *Advanced Mathematical Methods for Scientists and Engineers;* McGraw-Hill: New York, NY, 1978.

Bergman, T. H. et al. *JOSA B* **1989**, *6* (11), 2249.

Bill, J. *Phys. Rev. A 73* **2006**, 053609.

Fortágh, J.; Zimmerman, C. *RMP* **2007**, *79*, 235.

Hinds, E. A.; Eberlein, C. *Phys. Rev. A 61* **2000**, 033614.

Hinds, E. A.; Eberlein, C. *Phys. Rev. A 64* **2001**, 039902(E).

Ince, E. L. *Ordinary Differential Equations;* Dover: New York, NY, 1956, p. 396.

Lesanovsky, I.; Schmelcher, P. *Phys. Rev. A 70* **2004**, 063604.

Potvliege, R.M. and Zehnlé, V. *Phys. Rev. A 63*, **2001**, 025601.

Sukumar, C. V.; Brink, D. M. *Phys. Rev. A 56* **1997**, 2451.

NO. OF
COPIES   ORGANIZATION

    1   DARPA
             ATTN DR. AMIT LAL
             3701 N FAIRFAX DR
             ARLINGTON VA 22203-1714

    1   DARPA
             ATTN DR. JAY LOWELL
             3701 N FAIRFAX DR
             ARLINGTON VA 22203-1714

TOTAL: 34 (1, ELEC, 2 CDS, 31 HCS)